



## Section 9. Breeder materials

# Displacement damage parameters for fusion breeder blanket materials based on BCA computer simulations

Dieter Leichtle \*

*Forschungszentrum Karlsruhe, Institute for Reactor Safety, P.O. Box 3640, D-76021 Karlsruhe, Germany***Abstract**

Based on the MARLOWE code, a refined binary collision approximation (BCA) simulation model has been developed which is particularly suited for light mass and polyatomic ionic solids in a fusion environment. Main features of the model are described, including appropriate extensions of the kinematical procedure and the ion–solid interactions. Defect yields from the simulated collision cascades are used for deriving displacement cross sections in Be, Li<sub>2</sub>O, Li<sub>2</sub>SiO<sub>3</sub>, Li<sub>2</sub>SiO<sub>4</sub> and Li<sub>2</sub>TiO<sub>3</sub>. Comparisons with standard results show that there is an energy dependence which is strongly correlated with the spectrum of primary knock-on atoms. In particular, for lithium ceramics the contribution of damage induced by secondary helium and tritium is remarkable even in a fast neutron flux. The total displacements per atom in a fusion demonstration reactor blanket obtained by means of BCA-simulation results is in general lower than NRT-values by about 30% for the lithium breeder materials, but higher by around 90% for beryllium. These differences can be attributed to differences of binding properties and crystalline structure of the respective material, which also influence the defect composition.

© 2002 Elsevier Science B.V. All rights reserved.

**1. Introduction**

Atomic displacements as defined in the framework of the displacements per atom (dpa) concept are commonly used as base input for measures of radiation exposure. Calculations of such parameters in light mass and polyatomic ionic materials suffer severely from limitations of the well-established NRT-Lindhard model [1], which are due to restrictions of the underlying physics and insufficiencies of the microscopic modelling of material properties.

To this end, a refined binary collision approximation (BCA) simulation model has been developed and used for the calculation of the primary defect state of collision cascades. These are initiated by different types of primary knock-on atoms (PKA) from neutron induced nuclear reactions. Their energy spectra have been obtained from evaluated nuclear data files.

**2. Simulation model**

The NRT-Lindhard model provides the number of defects  $N_d$  in a PKA-initiated collision cascade using the damage energy  $E_{dam}$  and a simple isotropic displacement threshold energy  $E_d$ . However, it is valid only for medium mass ions at low energy in similar monatomic and amorphous targets. Furthermore, crystalline properties are not accounted for. Therefore, one may rely on direct atomistic computer simulations of the collision cascades. The most rigorous method, the molecular dynamics (MD), however, is excluded since we are dealing with kinetic energies of the light mass particles up to some MeV/amu, where MD would need forbiddingly large computing times. On the other hand, the BCA [2] is much more efficient by separating the cascade into binary encounters and asymptotic trajectories. The BCA-method breaks down at low energies where many-body effects come into play. These are excluded in principle, nevertheless, they can be approximated by using crystal binding energies and an appropriate treatment of quasi-simultaneous encounters.

\* Tel.: +49-7247 82 2557; fax: +49-7247 82 3718.

E-mail address: [leichtle@irs.fzk.de](mailto:leichtle@irs.fzk.de) (D. Leichtle).

The widely used BCA-code MARLOWE [3] was selected as the base for developing a BCA-model appropriate for polyatomic, light mass and ionic materials. It has been extended and modified including the implementation of high energy projectile-target interactions (up to some MeV/amu), a refined and extended modelling of target materials, a revised scheme of BCA and quasi-simultaneous encounters and finally, new routines of defect identification and characterisation. Major effort was devoted to the treatment of ionic compounds and its implications. Details of the model may be found in [4].

In ionic compounds attractive and long range forces (partly screened Coulomb-potentials) have to be considered. In principle this is unfeasible in a BCA-treatment due to the inherent restriction to solely binary collisions with a nearest target atom and the asymptotic calculations of particle trajectories. Therefore a model to describe partly screened Coulomb-potentials has been developed and implemented successfully into MARLOWE. Besides the selection of a suitable parameterisation of the screening function based on the AMLJ-potential [5], modifications of the BCA itself have to be performed including the determination of the apsis of the collision and the forced convergence of the time integral by using a cut-off distance.

Nonlocal and local inelastic energy losses are calculated using an interpolation scheme to bridge the low-energy velocity-dependent LSS stopping power of Lindhard et al. [6] to the Bethe–Bloch formula above 200 keV/amu. The radial dependence of local losses has been fitted to the maximum impact parameter available. In this work we have adopted a semi-empirical procedure [7] to correct Bragg values of compound stopping powers down to about 1 keV/amu.

The local binding model implemented in this work separates metallic, covalent and ionic contributions. Individual relative shares from neighbouring atoms can be specified to allow for definition of mixed bonding, like ionic–covalent. In our model the change of binding energy is due to missing or improper neighbouring lat-

tice atoms taking into account bond-strengthening effects in metallic and polarity in ionic bonds.

According to the needs presented above, the BCA-model in MARLOWE has been modified as follows. Improved formulations of collision integrals are introduced allowing for inelastic kinematics of binary collisions. A treatment of attractive potentials, which can influence the trajectories of particles, is incorporated to cope with more close encounters and even retrograde motion. Finally, as a consequence also of the target modelling, a newly revised scheme for quasi-simultaneous encounters has been developed.

### 3. Collision cascades in beryllium and lithium breeder ceramics

Simulations with the improved MARLOWE model have been performed for the neutron multiplier Be and the lithium breeder ceramics  $\text{Li}_2\text{O}$ ,  $\text{Li}_2\text{SiO}_3$ ,  $\text{Li}_4\text{SiO}_4$  and  $\text{Li}_2\text{TiO}_3$ . Selected material parameters relevant for the BCA-simulations are listed in Table 1. Note, that the model for  $\text{Li}_2\text{TiO}_3$  has been improved [4] compared to that one used in [8] with regard to the crystalline model and binding energies. Whereas the binding energy of Be is given explicitly in the literature, see e.g. [9], those of the breeder materials are derived from the heat of formation, taking into account the respective coordination of each lattice site. Thermal expansion of the lattices and uncorrelated thermal vibrations of the atoms at representative temperatures are also included.

In general, the cascade morphologies in these light mass materials tend to be more dilute and widespread. A typical cascade structure consists of one or a few tube-like tracks with isolated defects and tree-like branching only in the final parts. Damage production in these cascades supports the damage energy concept, since  $E_{\text{dam}}$  and  $N_{\text{d}}$  are correlated nearly linearly. Quantitative differences between the simulations and NRT, however, can be seen, in particular at higher energies and for the low mass PKAs. Also the effective displacement threshold energy  $Q = E_{\text{dam}}/N_{\text{d}} = 2.5E_{\text{d}}$  shows a remark-

Table 1  
Properties of fusion breeder blanket materials used for BCA-simulations

	$\text{Li}_2\text{O}$	$\text{Li}_2\text{SiO}_3$	$\text{Li}_4\text{SiO}_4$	$\text{Li}_2\text{TiO}_3$	Be
Crystal structure	fcc, Fm3m	orthorhombic, Cmc2 <sub>1</sub>	monoclinic, P2 <sub>1</sub> /m	monoclinic, C2/c	hcp, P6 <sub>3</sub> /mmc
Lattice constants (Å)	$a = 4.676$	$a = 9.49$ $b = 5.46$ $c = 4.71$	$a = 5.217$ $b = 6.31$ $c = 5.41$ $\beta = 90.27^\circ$	$a = 5.041$ $b = 8.806$ $c = 9.726$ $\beta = 100.008^\circ$	$a, b = 2.311$ $c = 3.615$
Binding energies (eV)	O = 6.2 Li = 3.1	Li = 1.5 O = 2.0 Si = 7.0	Li = 1.5 O = 2.0 Si = 7.0	Li = 2.9 O = 5.7 Ti = 11.5	Be = 3.3

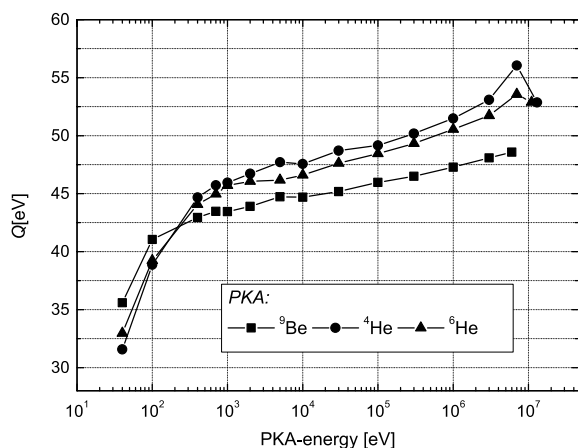


Fig. 1. Effective threshold for defect production in  ${}^9\text{Be}$  as function of PKA-energy.

able dependence on PKA-type and energy (see e.g. Fig. 1). Both findings are substantially different from NRT-predictions and can be attributed to crystalline properties of the respective solid.

To be more specific, the displacement of a central tetrahedral ion (like Si in  $\text{Li}_4\text{SiO}_4$  and Ti in  $\text{Li}_2\text{TiO}_3$ ) is strongly suppressed since it has to break through a shell of neighbouring ions. Its effective threshold value is quite large, i.e. 118 eV for Si and 162 eV for Ti. On the opposite, the more open fcc structure of  $\text{Li}_2\text{O}$  allows for easy displacement of the light mass constituent Li. Also the peculiar feature of partially occupied Li-sites in  $\text{Li}_4\text{SiO}_4$  favours defect annihilation of Li interstitials, reducing the value of  $Q$ .

#### 4. Displacement damage

To calculate the displacement damage cross section and the rate of displacements dpa/s one needs to have the energy spectra of all relevant recoil atoms or secondary light particles. They have been calculated with NJOY [10] and cross-section data mainly from ENDF/B-VI (plus selected evaluations from EFF2.4 and JENDL/FF3.2). In the case of beryllium we have used  ${}^9\text{Be}$ ,  ${}^4\text{He}$ ,  ${}^6\text{He}$  and  ${}^{10}\text{Be}$  from elastic scattering,  $(n, 2n)$ ,  $(n, \alpha)$  and  $(n, \gamma)$ . For the lithium breeder materials the following reactions have been taken into account: Elastic and inelastic scattering,  ${}^6\text{Li}(n, t)\alpha$ ,  ${}^{28}\text{Si}(n, p){}^{28}\text{Al}$ ,  ${}^{28}\text{Si}(n, \alpha){}^{25}\text{Mg}$ ,  ${}^{\text{nat}}\text{Ti}(n, 2n){}^{\text{nat}}\text{Ti}$ . Besides the heavy recoil atoms, the light tritium and helium particles produced mainly by the tritium breeding reaction in  ${}^6\text{Li}$  contribute significantly to the damage production in spite of their low mass. This is due to the fact, that the nuclear cross section is dominant below some keV and both particles are receiving kinetic energies above 2 MeV. In addition, owing to their high kinetic energy the defect morphology

of their cascades is track-like with isolated point defects, which is very distinct. Because of these reasons the  ${}^6\text{Li}$ -enrichment is of primary importance in dpa calculations and damage correlation analyses [11].

Combining now PKA energy spectra and damage production from the BCA simulations one arrives at displacement cross-sections  $\sigma_D(E)$  presented in Figs. 2 and 3 for the lithium breeder materials at a common  ${}^6\text{Li}$ -enrichment of 30 at.% and beryllium, respectively. In general, two regimes for the lithium breeder materials can be distinguished, a low-energy regime below some keV with the characteristic  $1/v$ -contribution of the exothermic  ${}^6\text{Li}(n, t)\alpha$ -reaction and a high-energy-regime dominated by the heavier PKAs. A similar characteristic shape can be recognized in the beryllium cross section,

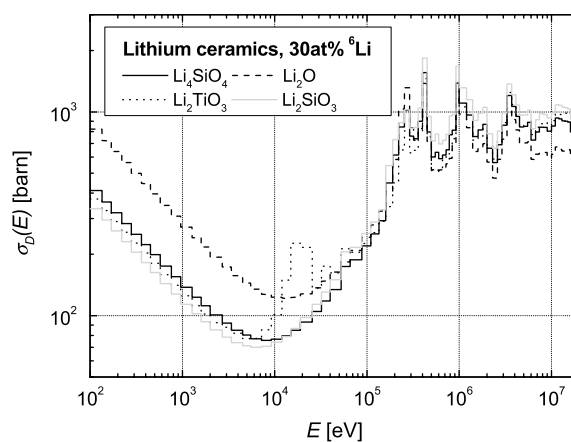


Fig. 2. Displacement cross-section of lithium breeder ceramics, enriched to 30 at.%  ${}^6\text{Li}$ .

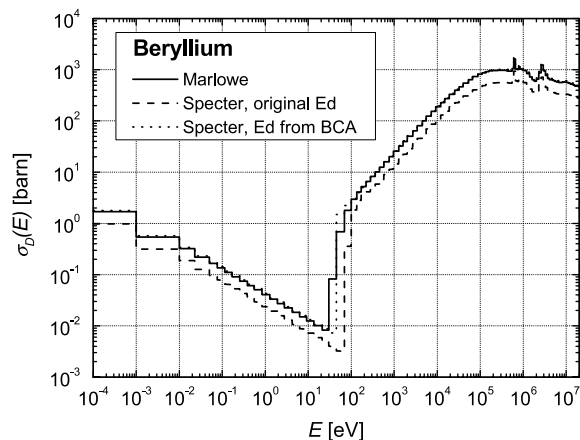


Fig. 3. Comparison of displacement cross sections of beryllium. SPECTER results are obtained by using  $E_d = 31$  eV ('original  $E_d$ ') and  $E_d = 17$  eV (' $E_d$  from BCA').

however, here the low energy part is due to neutron capture where the  $^{10}\text{Be}$ -nucleus receives a kinetic energy of roughly 2 keV from gamma emission. The elastic scattering contribution is most prominent, while the lighter recoils from  $(n, 2n)$  and  $(n, \alpha)$  provide only up to 10% above some MeV.

Since the damage production of the light mass PKA is much more affected by the BCA simulations than that of heavy mass PKAs the same is true for the resulting displacement cross sections. Examples are presented in Figs. 3 and 4, where the NRT-results are calculated with the damage codes SPECTER/SPECOMP [12,13].

In the case of beryllium the MARLOWE cross section exceeds the SPECTER cross section (with standard threshold energy) by about 90% over the entire energy range indicating the weak influence of low mass PKAs. Averaging the effective threshold energy  $Q$  over neutron energy results in an  $E_d$ -value of 17 eV for Be. Using this parameter in SPECTER leads to the curve labelled 'SPECTER,  $E_d$  from BCA' in Fig. 3. As can readily be seen, in this case the correspondence with MARLOWE is nearly perfect.

When looking at the displacement cross sections of the lithium breeder materials the differences in the low

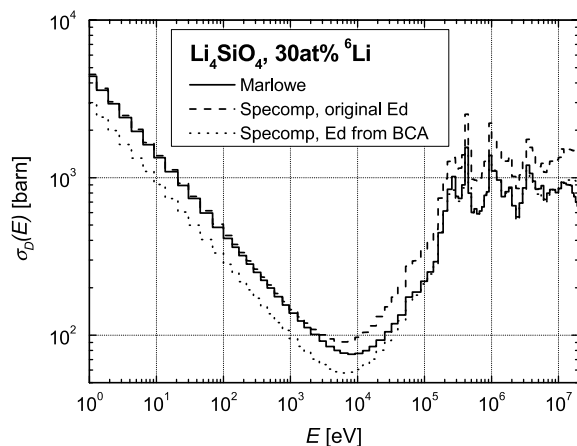


Fig. 4. Comparison of displacement cross sections of  $\text{Li}_4\text{SiO}_4$  (enriched to 30 at.%  $^6\text{Li}$ ). SPECOMP results are obtained by using its own threshold values ('original  $E_d$ ') and using those values, as derived by the present BCA simulations.

energy regime between SPECOMP and MARLOWE results are surprisingly moderate, in the range of  $-3\%$  for the lithium silicates,  $+10\%$  for  $\text{Li}_2\text{O}$  and  $+35\%$  for  $\text{Li}_2\text{TiO}_3$ . However, this is an artefact of the light particle's treatment within SPECTER/SPECOMP. Relying on a correct NRT-Lindhard formalism the mentioned differences are increased appreciably, e.g. in the case of  $\text{Li}_2\text{TiO}_3$  [14] up to  $+105\%$ .

At higher energies the MARLOWE results are in general lower than SPECOMP results, where the difference strongly correlates with resonances of particular PKAs. On the average the MARLOWE cross sections are reduced by about 35% for all of the breeder materials considered. Using derived threshold energies from the BCA simulations in SPECTER/SPECOMP usually gives a somewhat better agreement with MARLOWE results. Nevertheless, the discrepancy between low and high energy regimes remains as expected, cf. Fig. 4 for the case of  $\text{Li}_4\text{SiO}_4$ .

Accordingly, dpa-results for different neutron spectra are affected in as much the two regimes are contributing. In a typical fusion first-wall spectrum of a DEMO reactor the results are given in Table 2. It can be stated that the BCA simulations lead to a reduction of roughly 30% for the breeder materials under consideration, but to an increase of about 90% for beryllium. As already mentioned, the share due to Helium and Tritium in the lithium breeder materials is significant and amounts to roughly 20% which is slightly less than their contribution to the total PKA spectrum.

## 5. Conclusions

A BCA-model was developed which is well suited for light mass and polyatomic ionic solids. Based on collision cascade simulations using this model, improved displacement cross sections for Be,  $\text{Li}_2\text{O}$ ,  $\text{Li}_2\text{SiO}_3$ ,  $\text{Li}_2\text{SiO}_4$  and  $\text{Li}_2\text{TiO}_3$  have been calculated and compared to standard NRT-results as supplied by the damage codes SPECTER/SPECOMP. While in the monatomic Be-lattice the difference is nearly independent on energy, the opposite is true for the polyatomic lithium breeder materials. This can be attributed to the variable impact of light and heavy mass PKAs, respectively, in particular to the role of helium and tritium from  $^6\text{Li}(n, t)\alpha$ .

Table 2

Dpa rates for fusion breeder blanket materials in a DEMO first-wall spectrum

Dpa/FPY	$\text{Li}_2\text{O}$ -30 at.% $^6\text{Li}$	$\text{Li}_2\text{SiO}_3$ -30 at.% $^6\text{Li}$	$\text{Li}_4\text{SiO}_4$ -30 at.% $^6\text{Li}$	$\text{Li}_2\text{TiO}_3$ -30 at.% $^6\text{Li}$	Be
MARLOWE	22.7	23.8	21.5	21.0	21.4
SPECOMP	30.4	32.1	32.3	31.3	11.2
$\Delta$ (MARLOWE relative to SPECOMP) (%)	-25	-26	-33	-33	+91

## Acknowledgements

This work has been performed in the framework of the Nuclear Fusion Project of the Forschungszentrum Karlsruhe and is supported by the European Communities within the European Fusion Technology Program.

## References

- [1] M.J. Norgett, M.T. Robinson, I.M. Torrens, Nucl. Eng. Des. 33 (1975) 50.
- [2] M.T. Robinson, Radiat. Eff. Def. 130&131 (1994) 3.
- [3] M.T. Robinson, Phys. Rev. B 40 (1989) 10717.
- [4] D. Leichtle, Nucl. Instrum. and Meth. B 180 (2001) 194.
- [5] S.T. Nakagawa, Radiat. Eff. Def. 116 (1991) 21.
- [6] J. Lindhard, V. Nielsen, M. Scharff, Mat. -fys. Medd. 33 (10) (1963).
- [7] D.I. Thwaites, Nucl. Instrum. and Meth. B 69 (1992) 53.
- [8] D. Leichtle, U. Fischer, Fus. Eng. Des. 51&52 (2000) 1.
- [9] Gmelin Handbuch der anorganischen Chemie, Beryllium Supplement A2, Springer, Berlin, 1991.
- [10] R.E. MacFarlane, D.W. Muir, R.M. Boicourt, The NJOY Nuclear Data Processing System, vol. I, User's Manual, Los Alamos National Laboratory, 1993, LA-12740-M.
- [11] U. Fischer, S. Herring, A. Hogenbirk, et al., J. Nucl. Mater. 280 (2000) 151.
- [12] L.R. Greenwood, R.K. Smither, SPECTER: Neutron damage calculations for materials irradiations, Argonne National Laboratory, 1985, ANL/FPP/TM-197.
- [13] L.R. Greenwood, SPECOMP calculations of radiation damage in compounds, in: H. Farrer, E.P. Lippincott (Eds.), Reactor Dosimetry: Methods, Applications, and Standardization, ASTM STP 1001, 1989, p. 598.
- [14] L.R. Greenwood, personal communication, December 1998.